A NUMERICAL SIMULATION FOR TSUNAMIS DUE TO A LANDSLIDE

Taro Kakinuma[1] and Tsunakiyo Iribe[2]

Tsunamis, generated by falling rigid bodies, have been numerically simulated using the MPS model, in the vertical two dimensions. The numerical result for the water surface displacement of the first wave is in harmony with the corresponding experimental result obtained using the cylinders. A tsunami component traveling toward the shore and running up the slope can be confirmed in the present cases. The tsunami height, immediately after the large circles enter the water, does not depend much on the offshore still water depth, while the tsunami-height reduction is suppressed, when the offshore still water depth is shallower. Conversely, the tsunami height, immediately after the small circles enter the water, increases as the offshore still water depth is shallower. Both the tsunami height, immediately after the falling bodies enter the water, and the reduction rate of tsunami height, are larger for the large circles than for the small circles. In the cases where the falling rigid bodies include both the large and small circles, the reduction rate of the water level near the tsunami source is larger, when the large circles are stacked on the offshore side at the initial condition.

Keywords: tsunami, landslide, rigid body, MPS method

INTRODUCTION

Tsunamis can be triggered by not only submarine earthquakes but also by landslides. In 1792, the tsunamis due to a landslide, or a sector collapse, at Mt. Mayu, Japan, traveled over the Ariake Sea, resulting in a runup on the opposite shore (Togashi and Hirayama, 1993). Such tsunamis are not necessarily generated only by soil or rocks: an excursion ship could be hit by tsunamis due to a partial collapse of glacier near a coast on Svalbard Islands, Norway (Marchenko et al., 2012). These tsunamis are generated through an interaction between water motion and falling bodies, such that the tsunami generation process is rather complicated.

Tsunami generation due to a landslide or a sector collapse has also been studied numerically with various methods, including a smoothed particle hydrodynamics (SPH) model (e.g. Panizzo and Dalrymple, 2005) and a moving particle semi-implicit (MPS) model (e.g. Gotoh et al., 2011). In the present study, we have investigated several fundamental characteristics of tsunami generation caused by a landslide, on the basis of results in two vertical dimensions, obtained through a numerical simulation based on an MPS model, where the falling body is assumed to be a group of rigid bodies, which move down a slope with a constant gradient.

NUMERICAL METHOD AND CONDITIONS

The Lagrangian model, developed by Iribe and Nakaza (2011), based on the MPS method designed by Koshizuka and Oka (1996), is applied to consider the furious water motion. The water level is determined using the spatial gradient of particle-number density, to inhibit pressure disturbance at the water surface. No turbulence model is utilized for fluid motion, and both fluid viscosity and surface tension are neglected. On the other hand, both the elasticity and the plasticity of falling bodies are neglected for simplicity. The interparticle distance is 0.002 m or 0.005 m in the present cases.

Figure 1 shows the target domain inside a water basin with a slope, where the gradient of the slope is 45°. The distance between the starting point of the slope and the offshore wall is 3.00 m, and the still water depth off the slope, h, is uniformly 0.09 m or 0.245 m. The origin of the coordinate axes is at the shoreline in the still water condition. The positive direction of the x-axis is the horizontal offshore direction, while the positive direction of the z-axis is the upward direction. In the hydraulic experiments, a vertical gate is opened quickly to reproduce a landslide, where the inner width of the basin is 0.2 m.

The release of objects, stacked on the slope, is the start of a landslide, or a sector collapse, to generate tsunamis, where the vertical gate is located at the initial position of the shoreline. In the cases where the falling body is water, both the wave height and the wave phase of the first wave, obtained using the MPS model, are in harmony with the experimental results (Kakinuma, 2016).

In the present study, the falling objects are assumed to be rigid bodies as follows:

[1] Graduate School of Science and Engineering, Kagoshima University, 1-21-40 Korimoto, Kagoshima, Kagoshima 890-0065, Japan
[2] Faculty of Engineering, University of the Ryukyus, 1 Sembaru, Nishihara-cho, Nakagami, Okinawa 903-0213, Japan

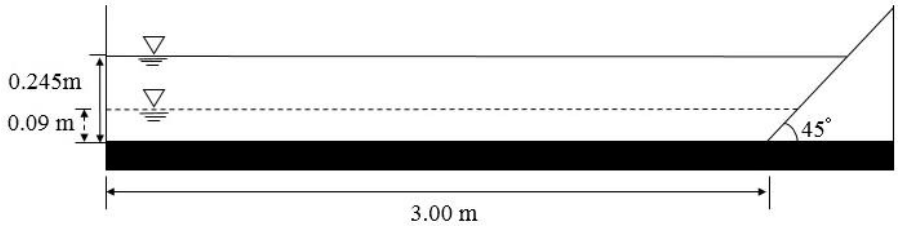

Figure 1. The target domain inside a water basin with a slope, where x = 0.0 m at the shoreline.

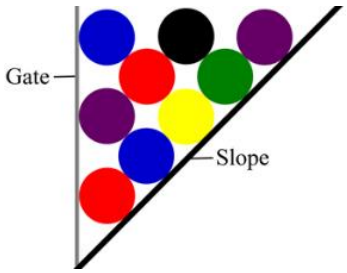

Figure 2. A sketch of the cylinders at the initial condition. The diameter and density of the cylinders are 2.0 cm and 2,300 kg/m^3, respectively.

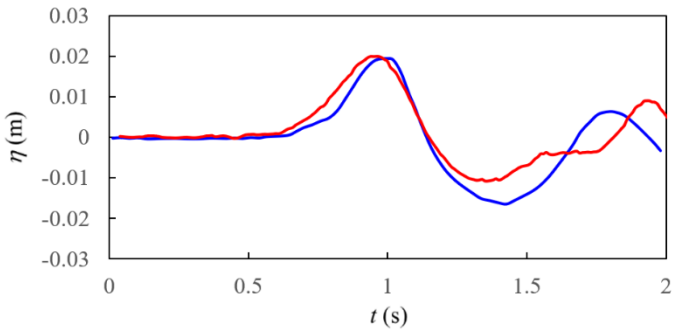

Figure 3. The water surface displacements at x = 0.7 m, where h = 0.09 m. The blue line represents the experimental result for the water surface displacement due to the falling rigid cylinders, while the red line shows the corresponding numerical result obtained using the MPS method, where the falling objects are the circles. The diameter and density of both the cylinders and the circles are 2.0 cm and 2,300 kg/m^3, respectively.

(1) Cylinder: In the hydraulic experiments, the diameter and length of cylinders are 2.0 cm and 0.197 m, respectively. The material of the cylinders is polytetrafluoroethylene (PTFE). In the vertically two-dimensional numerical calculation, a cylinder is assumed to be a circle, which consists of 12 rigid particles, where the interparticle distance is 0.002 m. The density is 2,300 kg/m^3.

(2) Large circle: The diameter of large circles is 2.0 cm. A large circle consists of 21 rigid particles, where the interparticle distance is 0.005 m. The density is 2,600 kg/m^3.

(3) Small circle: The diameter of small circles is 0.5 cm. A small circle consists of 4 rigid particles, where the interparticle distance is 0.005 m. The density is 2,600 kg/m^3.

Conversely, the density of water is 1,000 kg/m^3 in the basin.

TSUNAMIS CAUSED BY FALLING CYLINDERS OR CIRCLES

Shown in Fig. 2 is the initial condition for a group of cylinders at t = 0.0 s, where the diameter and density of the cylinders are 2.0 cm and 2,300 kg/m^3, respectively. Figure 3 shows the water surface displacements at x = 0.7 m, where h = 0.09 m and the initial condition of the falling bodies is shown in Fig. 2. The blue line represents the experimental result for the water surface displacement due to the falling rigid cylinders, while the red line shows the corresponding numerical result obtained using the

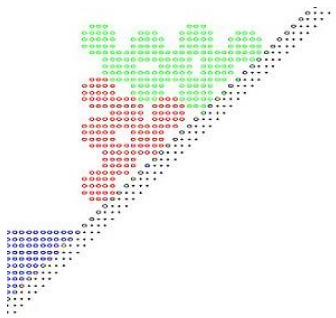

Figure 4. A sketch of the large circles at the initial condition. The diameter and density of the circles are 2.0 cm and 2,600 kg/m^3, respectively.

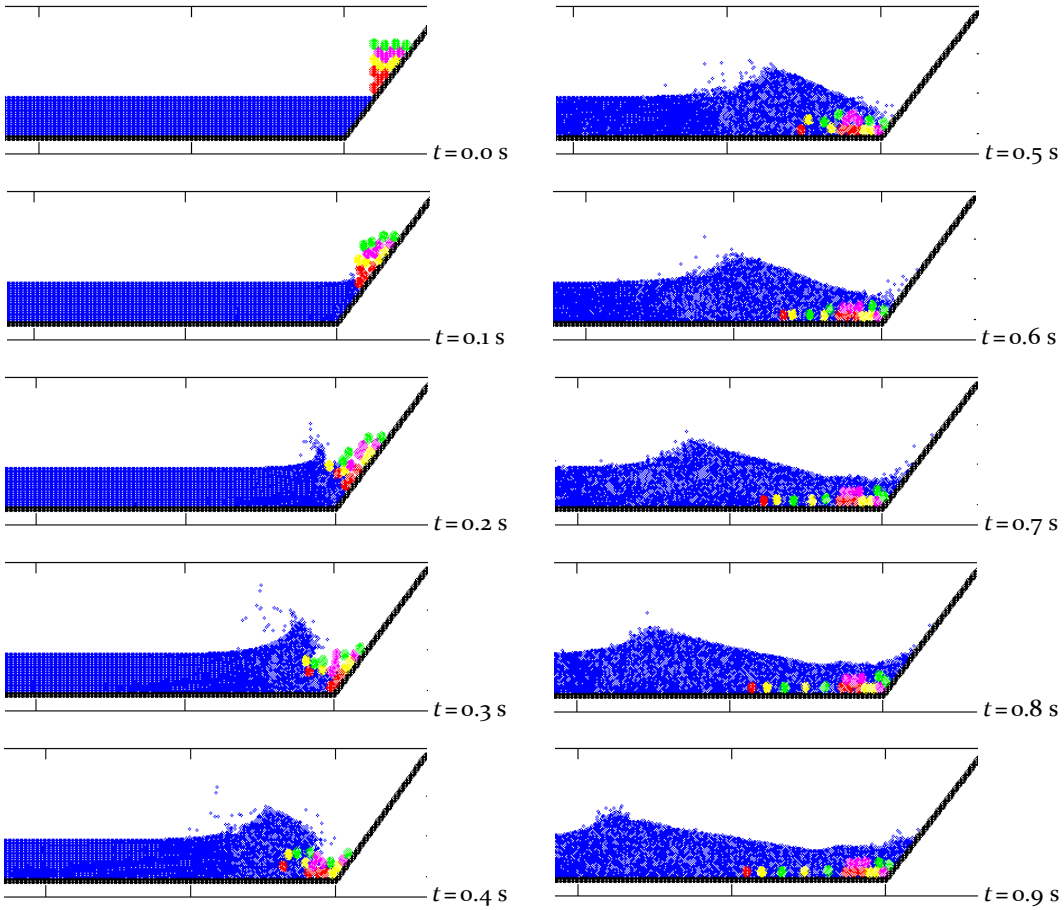

Figure 5. The numerical simulation result for the tsunamis caused by the falling large circles, where *h* = 0.09 m and the initial condition of the falling bodies is shown in Fig. 4.

MPS method, where the falling objects are the circles. The diameter and density of both the cylinders and the circles are 2.0 cm and 2,300 kg/m3, respectively. The water surface displacement of the first wave obtained using the MPS model is in harmony with the experimental result, although future work is required to calculate the behavior of the circles in water more accurately to reproduce the second wave.

In another case, as shown in Fig. 4, 16 large circles are arranged on the slope at the initial time t = 0.0 s, where the diameter and density of the circles are 2.0 cm and 2,600 kg/m^3, respectively. Figure 5 shows the numerical simulation result, where the offshore still water depth h is 0.09 m. After the generation of the first wave, part of the water runs up on land, such that it is necessary to consider the tsunami component that travels toward the shore, when tsunamis are caused by a nearshore landslide whether the landslide begins above or below the sea level.

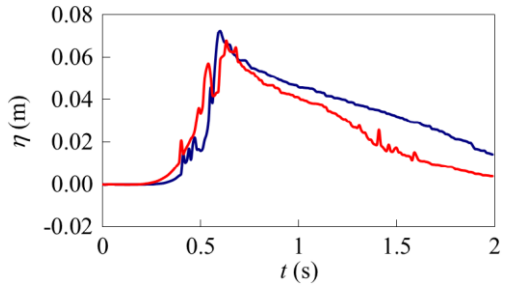

(a) x = 0.6 m

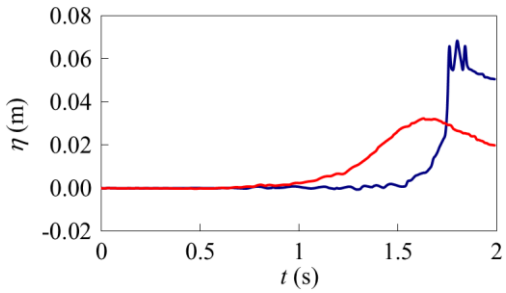

(b) x = 2.15 m

Figure 6. The water surface displacements due to the falling large circles at x = 0.6 m and 2.15 m, where the initial condition of the falling bodies is shown in Fig. 4. The blue and red lines represent the numerical results when h = 0.09 m 0.245 m, respectively.

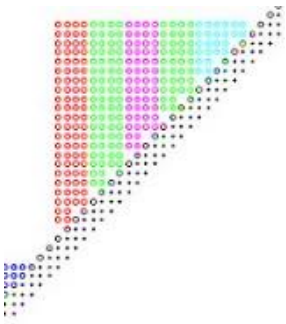

Figure 7. A sketch of the small circles at the initial condition. The diameter and density of the circles are 0.5 cm and 2,600 kg/m^3, respectively.

Shown in Fig. 6 are the water surface displacements at x = 0.6 m and 2.15 m, where the uniform still water depth off the slope, h, is 0.09 m or 0.245 m. The tsunami height is defined as the maximum value of water surface displacement at each location. According to Fig. 6(a), the tsunami height at x = 0.6 m is 0.072 m when h = 0.09 m, and 0.068 m when h = 0.245 m, such that the difference between these cases is not large, that is, the tsunami height, immediately after the large circles enter the water, does not depend much on the still water depth. Conversely, according to Fig. 6(b), the tsunami height at x = 2.15 m is 0.066 m when h = 0.09 m, and 0.032 m when h = 0.245 m, such that the tsunami-height reduction rate differs greatly for the two cases, for the reduction in the tsunami height is suppressed owing to shallowing, showing the steeper wave front, in the former with the shallower offshore still water depth.

TSUNAMIS CAUSED BY FALLING SMALL CIRCLES

As indicated in Fig. 7, 66 rigid small circles are placed on the slope at the initial time t = 0.0 s. Both the total mass, and the vertical position of the center of gravity at t = 0.0 s, of all the small circles are equal to those of all the large circles shown in Fig. 4. Shown in Fig. 8 are the water surface displacements at x = 0.6 m and 2.5 m. According to Fig. 8(a), the tsunami height at x = 0.6 m is 0.061 m when h = 0.09 m, and 0.046 m when h = 0.245 m, such that there is a difference in the tsunami height, immediately after the small circles enter the water, where the tsunami height increases as the offshore still water depth

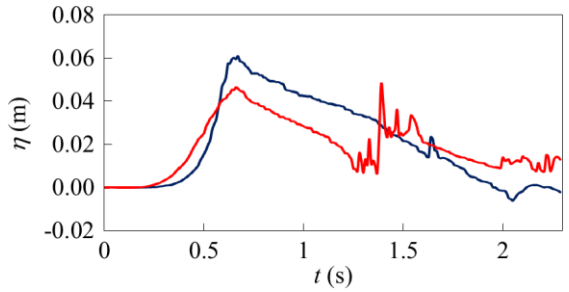

(a) x = 0.6 m

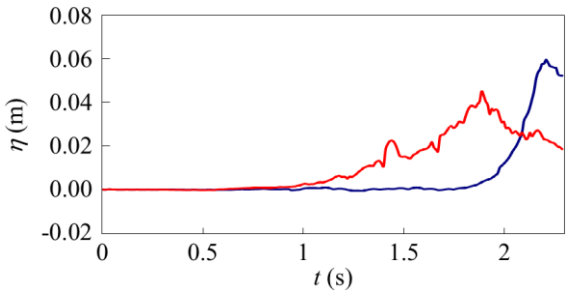

(b) x = 2.5 m

Figure 8. The water surface displacements due to the falling small circles at x = 0.6 m and 2.5 m, where the initial condition of the falling bodies is shown in Fig. 7. The blue and red lines represent the numerical results when h = 0.09 m 0.245 m, respectively.

is shallower. It should be noted that the second wave, reflected on the slope, remarkably appears in the deeper case, at $t \simeq 1.4$ s.

According to Figs. 6(a) and 8(a), the tsunami height, immediately after the rigid bodies enter the water, is larger when the falling bodies are the large circles than when those are the small circles, for more water can enter between the small circles. Conversely, according to Fig. 8(b), the tsunami height at x = 2.5 m is 0.060 m when h = 0.09 m, and 0.045 m when h = 0.245 m, such that the reduction rate of tsunami height is lower for the falling small circles than for the falling large circles.

TSUNAMIS CAUSED BY FALLING RIGID BODIES INCLUDING BOTH LARGE AND SMALL CIRCLES

Shown in Fig. 9 are the initial conditions for a group of rigid bodies, including circular bodies of different diameters, i.e., 2.0 cm and 0.5 cm. Figure 10 shows the water surface displacements at x = 0.6 m, where h = 0.09 m. Although there is no significant difference in the tsunami height for these cases immediately after the falling bodies plunge into the water, the reduction rate of the water level at this location is larger when the large circles are also stacked on the offshore side at the initial condition.

CONCLUSIONS

The tsunamis, generated by the falling rigid bodies, were numerically simulated using the MPS model, in the vertical two dimensions. The numerical result for the water surface displacement of the first wave was in harmony with the corresponding experimental result obtained using the cylinders.

A tsunami component traveling toward the shore and running up the slope was confirmed in the present cases.

The tsunami height, immediately after the large circles entered the water, did not depend much on the offshore still water depth, while the tsunami-height reduction was suppressed, when the offshore still water depth is shallower. Conversely, the tsunami height, immediately after the small circles entered the water, increased as the offshore still water depth was shallower. Both the tsunami height, immediately after the falling bodies entered the water, and the reduction rate of tsunami height, were larger for the large circles than for the small circles.

In the cases where the falling rigid bodies included both the large and small circles, the reduction rate of the water level near the tsunami source was larger, when the large circles are stacked on the offshore side at the initial condition.

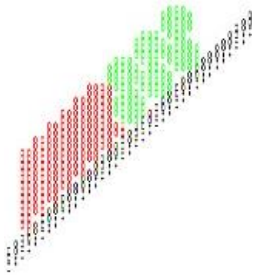

(a) The large circles are on the onshore side.

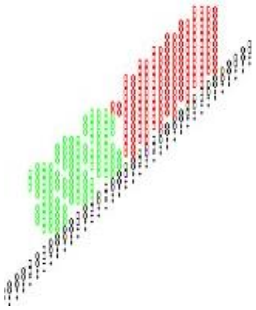

(b) The large circles are on the offshore side.

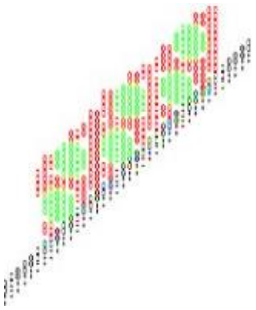

(c) The large and small circles are mixed.

Figure 9. Sketches of the initial conditions for the falling rigid bodies, including both the large and small circles, the diameter of which is 2.0 cm and 0.5 cm, respectively.

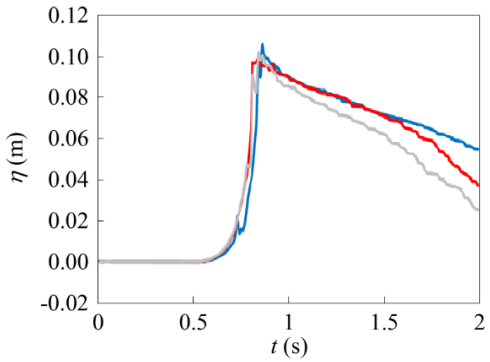

Figure 10. The water surface displacements at x = 0.6 m, due to the falling rigid bodies including both the large and small circles, where h = 0.09 m. The blue line represents the water surface displacement when the large circles are initially arranged on the onshore side, as shown in Fig. 9(a); the red line when the large circles are initially stacked on the offshore side, as shown in Fig. 9(b); the gray line when the large and small circles are mixed at the initial condition, as shown in Fig. 9(c).

ACKNOWLEDGMENTS

Sincere gratitude is extended to Ms. Manami Higashi, Ms. Aya Oyama, Mr. Ryo Sawada, and Mr. Mitsuru Yanagihara, who contributed to the numerical simulation, as well as the hydraulic experiments, when they were students at Kagoshima University.

The authors also express our gratitude to Mr. Kuninori Nagai, University of the Ryukyus, who cooperated in the numerical calculation.

REFERENCES

Gotoh, H., H. Ikari, T. Matsubara, T. Ito. 2011. Numerical simulation on tsunami due to sector collapse by solid-liquid two-phase flow model based on accurate particle method. *J. JSCE B2 (Coastal Eng.)*, 67(2), I_196-I_200 (in Japanese with an English abstract).

Iribe, T. and E. Nakaza. 2011. An improvement of accuracy of the MPS method with a new gradient calculation model, *J. JSCE, B2 (Coastal Eng.)*, 67(1), 36-48 (in Japanese with an English abstract).

Kakinuma, T. 2016. Tsunami generation due to a landslide or a submarine eruption, *In: Tsunami (Ed. Mokhtari)*, InTech, 35-58.

Koshizuka, S. and Y. Oka. 1996. Moving-particle semi-implicit method for fragmentation of incompressible fluid, *Nucl. Sci. Eng.*, 123, 421-434.

Marchenko, A. V., E. G. Morozov, S. V. Muzylev. 2012. A tsunami wave recorded near a glacier front, *Nat. Hazards Earth Syst. Sci.*, 12, 415-419.

Panizzo, A. and Dalrymple, R. A. 2005. SPH modelling of underwater landslide generated waves, *Coastal Eng. 2004 (Ed. Smith, J. M.)*, ASCE, 1147-1159.

Togashi, H. and Hirayama, Y. 1993. Hydraulic experiment on reappearance of the Ariake-kai tsunami in 1792, *Proc. IUGG/IOC Int. Tsunami Symp. (Tsunami '93)*, 741-754.